

# LEARNING TRANSFER OPERATORS BY KERNEL DENSITY ESTIMATION

Sudam Surasinghe <sup>1,2,3\*</sup>, Jeremie Fish <sup>1,†</sup> and Erik M. Bollt <sup>1,‡</sup>

<sup>1</sup> *Department of Ecology and Evolutionary Biology, Yale University, New Haven, CT, 06520 USA*

<sup>2</sup> *Public Health Modeling Unit, Yale School of Public Health, New Haven, CT 06510 USA*

<sup>3</sup> *Clarkson Center for Complex Systems Science, Department of Electrical and Computer Engineering, Clarkson University, 8 Clarkson Ave, Potsdam, New York 13699, USA*

\* *sudam.surasinghe@yale.edu*

† *fishja@clarkson.edu*

‡ *ebollt@clarkson.edu*

Inference of transfer operators from data is often formulated as a classical problem that hinges on the Ulam method. The usual description, which we will call the Ulam-Galerkin method, is in terms of projection onto basis functions that are characteristic functions supported over a fine grid of rectangles. In these terms, the usual Ulam-Galerkin approach can be understood as density estimation by the histogram method. Here we show that the problem can be recast in statistical density estimation formalism. This recasting of the classical problem, is a perspective that allows for an explicit and rigorous analysis of bias and variance, and therefore toward a discussion of the mean square error.

*Keywords:* Transfer Operators; Frobenius-Perron operator; probability density estimation; Ulam-Galerkin method; Kernel Density Estimation (KDE).

## 1. Introduction

Transfer operators play a vital role in the global analysis of dynamical systems. The availability of large amounts of data from dynamical systems drives the popularity of these operators in data-driven analysis methods for complex systems. Therefore, accurately estimating the transfer operators from data is crucial for successful global analysis. Frobenius-Perron operator is one such popular operator used for global analysis of dynamical systems, and the Ulam method [Ulam, 1960] is the most popular method to estimate it [Hunt, 1998; Ermann & Shepelyansky, 2010; Junge & Koltai, 2009; Hunt, 2000; Froyland *et al.*, 2013]. However, as we point out here, there are tremendous opportunities to recast this problem as one of density estimation as would be stated in the statistics literature. This approach offers a well-developed analysis of variance and bias, enabling discussions of mean squared error. This language has been overlooked in the dynamical systems community. Therefore, here we introduce the probability density estimation viewpoint to estimating the Frobenius-Perron operator, and with it the rich analysis already developed in other mathematical communities and methods, notably kernel estimation which as it turns out is provably more efficient than the histogram methods used in the standard Ulam method. Also, note that while kernel regression methods are commonly used in operator estimation problems, such as Koopman operators ([Klus *et al.*, 2018a, 2019, 2018b; Mollenhauer *et al.*, 2020]), kernel density estimation is a distinct technique.

A Frobenius-Perron operator evolves the density of ensembles of initial conditions of a dynamical system forward in time. This statement can also be re-interpreted in a Bayesian framework. Hence, we argue that we have essentially a problem of density estimation for the conditional probability density that

is generally described as the Frobenius-Perron operator. Therefore, the classical Ulam method is essentially a histogram method for the estimation of this conditional density function by simple nonparametric means. Many, including one of the authors of this work, have described the approach as a projection onto basis functions as characteristic functions, and in these terms, we described it as Ulam-Galerkin's method [Bollt & Santitissadeekorn, 2013], which covers many of the analyses of convergence since the original conjecture [Chiu *et al.*, 1992; Boyarsky & Góra, 1997; Dellnitz *et al.*, 2001; Guder *et al.*, 1997].

However, it is generally understood that histograms, while easy to describe, are a primitive variant amongst the approaches available to the problem of nonparametric density estimation. It has been said by Tukey [Tukey, 1961; Tukey & Tukey, 1981], that appearance of the traditional histogram is blocky, and difficult to balance smoothing, bandwidth, bias, and variance. Even in two dimensions, “blocky” variability of sampling, and details such as the simply choosing an appropriate orientation of the grid, become problematic. There are, however, more suitable methods that are reviewed here, especially the KDE which has many nice smoothing, analytic, and convergence properties. Additionally, density estimation is shifted from a question of density in space to expectation of points. Note also that the k-nearest neighbor (kNN) methods also have many of these advantages, but kernel methods allow for better tuning of smoothing parameters and good convergence statistics.

It is argued in [Dehnad, 1987], that the argument for KDE instead of a simple histogram method becomes stronger in more than one dimension, due to difficulties not only in histogram box size (bandwidth) but now also, in orientation and origin location that generally lead to a block appearance that becomes more difficult to interpret the joint and conditional probabilities. Tukey asserted [Tukey & Tukey, 1981], “...it is difficult to do well with bins in as few as two dimensions. Clearly, bins are for the birds!”

In this article, we aim to provide a comprehensive analysis of the density estimation approach for estimating the Frobenius-Perron operator. We begin by discussing the standard theory for the operator and the classical Ulam-Galerkin method in Section 2. Using Bayesian theory (in Section 3), we then analyze the Ulam method as a histogram-based density estimation technique and argue for the use of a standard density estimation approach for estimating the Frobenius-Perron operator. We demonstrate the theoretical advantages of kernel density estimation over the histogram-based Ulam method, particularly in terms of variance and bias. We also provide a detailed analysis of the convergence properties of kernel density estimation. Finally, we apply our theoretical analysis to the well-known chaotic logistic map example in Section 5. By comparing the accuracy of the kernel density estimation approach to the Ulam method, we demonstrate the superior performance of the former in estimating the Frobenius-Perron operator.

Overall, our study highlights the benefits of adopting a standard density estimation approach for estimating transfer operators, particularly in the context of data-driven analysis methods for complex systems. By recasting the problem of estimating the Frobenius-Perron operator as a density estimation problem, we can leverage the well-developed theory and methods in the statistics literature to improve the accuracy and efficiency of the estimation process. In order to maintain consistency with standard notation used in the statistics literature [Silverman, 1999; Scott, 2015], we will adopt the symbols commonly used in density estimation theory. The Table 1 shows the symbols that will be used throughout this article.

## 2. Frobenius-Perron and the Classical Ulam-Galerkin Method for Estimation

First we briefly review a standard discussion of Frobenius-Perron operators for deterministic and then random maps, and flows are covered in as much as the maps discussed can be taken as derived from the flow by a Poincaré or stroboscopic mapping. Assuming a map,

$$\begin{aligned} f : \Omega &\rightarrow \Omega, \\ x &\mapsto f(x), \end{aligned} \tag{1}$$

the forward orbit of initial condition  $x$ ,  $\text{orbit}(x) = \{x, f(x), f^2(x), \dots\}$  is a fundamental object in the study of dynamical systems. However, if we consider an ensemble of many initial conditions, that are distributed by  $\rho \in L^1(\Omega)$ , and we assume  $f$  is a nonsingular transformation and measurable relative to  $(\Omega, \mathcal{B}, \mu)$  on a Borel sigma-algebra of measurable sets  $\mathcal{B} \subset \Omega$  with measure  $\mu$ , then follows the Frobenius-Perron operator that describes the orbit of ensembles( here we are following our notation from [Bollt & Santitissadeekorn,

Table 1. List of Symbols: Throughout the article, we will use these symbols to denote the relevant quantities and functions.

Symbol	Description
$\Omega$	state space of a map $f$
$f$	map $f : \Omega \rightarrow \Omega$ such that $x \mapsto f(x)$
orbit	orbit of a dynamical system $f$
$X$	Random Variable
$X'$	transformed random variable such that $X' = f(X)$
$\rho_X, p_X$	Probability Density Function of random variable $X$
$\bar{p}_\theta$	Estimated Probability Density Function with parameter $\theta$
$\mathcal{P}$	Frobenius-Perron operator
$\mathbf{P}$	Matrix approximation to the Frobenius-Perron operator
$B_i$	$i^{th}$ bin or box such that $\mathcal{B} = \{B_i\}_{i=1}^K$ , $K > 0$ is a finite topological cover of $\Omega$
$\mathcal{K}$	Kernel in a KDE
MSE	Mean Square Error
UB	Upper Bound
bias	bias of the estimator
Var	Variance
erf	Gauss error function

2013], and comparable to [Lasota & Yorke, 1982]). The linear map,  $\mathcal{P}_f : L^1(\Omega) \rightarrow L^1(\Omega)$ , follows the discrete continuity equation,

$$\int \rho_{n+1} d\mu = \int_{f^{-1}(B)} \rho_n d\mu, \text{ for any } B \in \mathcal{B}. \quad (2)$$

For differentiable maps, this simplifies ,

$$\mathcal{P}_f[\rho](x) = \sum_{y: x=f(y)} \frac{\rho(y)}{|Df(y)|}, \quad (3)$$

where if  $f(y)$  is a single-variate function, then  $|Df(y)| = |f'(y)|$  is the absolute value of the derivative, or it is the determinant of the Jacobain (matrix) derivative if multi-variate. The following equivalent form is relevant for our purposes here,

$$\mathcal{P}_f[\rho](x) = \int_X \delta(x - f(y)) \rho(y) dy, \quad (4)$$

in terms of the delta function. Also, we have specialized to Lebesgue measure on  $\Omega$  from this point forward.

The Ulam-Galerkin method is a way to estimate the action of the Frobenius-Perron operator, given a (fine) finite topological cover of  $\Omega$  by (usually rectangles, or boxes, or triangles, or other simple spatial elements)  $\mathcal{B} = \{B_i\}_{i=1}^K$ ,  $K > 0$ . The matrix approximation  $\mathbf{P}$  is defined as follows:

$$\mathbf{P}_{i,j} = \frac{m(B_i \cap f^{-1}(B_j))}{m(B_i)}, \quad (5)$$

where  $m(B) = \int_B dx$  represents the Lebesgue measure. In fact, a simple estimate of this  $K \times K$  matrix  $\mathbf{P}$  follows if a large collection of input, output pairs are available,  $(x_n, x_{n+1})$ , as examples of  $x \in B_i \cap f^{-1}(B_j)$  perhaps derived from a long orbit that samples the space. Note that  $f^{-1}$  denotes the pre-image of  $f$  which may well not be one-one. This estimate is given by:

$$\mathbf{P}_{i,j} \sim \frac{\#x_n \in B_i, x_{n+1} \in B_j}{\#x_n \in B_i}. \quad (6)$$

Notice that the “ $\cap$ ” notation for intersection of sets is coincident with the “,” notation for “and” which denotes both events occur. This is useful for reinterpretation by a Bayesian discussion in the next section. Under the above construction, it can easily be seen that  $\mathbf{P}$  is a stochastic matrix, which therefore has

a leading eigenvalue of 1 and, if simple, a dominant eigenvector which describes the steady state of the corresponding Markov chain.

The original Ulam-conjecture [Ulam, 1960] described that, in a limit of a refining partition  $\{B_i\}$ , the dominant eigenvector of the discrete state Markov chain converges to invariant density of the original dynamical system. This conjecture was first proved by Li [Li, 1976] under hypothesis of bounded variation of one-dimensional maps, providing weak convergence.

An estimate such as Equations (5) and (6) has previously been called an Ulam-Galerkin estimate [Bollt & Santitissadeekorn, 2013; Ma & Bollt, 2013], a description which we made to intentionally separate the concept of the limit of long time iteration, as one does when considering ergodic averages, from short time considerations, such as that Equations (5) and (6) can simply be taken as an estimate of the action of the map on ensemble densities, between two time frames, or perhaps to be iterated a few times. The phrase Galerkin is stated in terms of projection of the action of the operator onto a basis of characteristic functions  $\{\xi_{B_i}(x)\}$ , supported over the grid elements,  $\{B_i\}$ ,

$$\xi_{B_i}(x) = \begin{cases} 1, & \text{if } x \in B_i \\ 0, & \text{otherwise} \end{cases} \quad (7)$$

Then the Ulam-Galerkin estimate formally describes a projection,  $R : L^2(\Omega) \rightarrow \Delta_K$ , for a finite linear subspace  $\Delta_K \subset L^2(\Omega)$ , that is spanned by the collection of characteristic functions over the grid elements. Notice, for this description, this is in terms of  $L^2(\Omega)$ , in order that an inner product structure makes sense, and then

$$\mathbf{P}_{i,j} = \frac{(\xi(B_i), \xi(f^{-1}(B_j)))}{\|\xi_{B_i}\|} = \frac{\int_X \xi(B_i)(x) \xi(f^{-1}(B_j)(x) dx}{\int_X \xi_{B_i}(x)^2 dx}. \quad (8)$$

If considering this finite rank transition for finite time discussion, then we worry only about the estimation of transitions by finite estimation by the basis functions as discussed in, [Bollt & Santitissadeekorn, 2013; Bollt *et al.*, 2002]. Infinite time questions are clearly more nuanced which is why the Ulam-conjecture remained a conjecture for almost twenty years. Our Bayesian discussion will likewise avoid the same.

In the more general case of a random dynamical system, Section 2 is recast,

$$x_{n+1} = f(x_n) + s_n, \quad (9)$$

which describes a deterministic part  $f$  together with a stochastic “kick”  $s$  which we assume is identically independently distributed by  $x \sim \nu$ . Consequently, the kernel integral form of the Frobenius-Perron transfer operator becomes,

$$\mathcal{P}_f[\rho](x) = \int_X \nu(x - f(y)) \rho(y) dy, \quad (10)$$

which we see is closely related to the zero-noise case of Equation (4) where the kernel in that case is a delta-function. For discussion in the next section, we will specialize further to the truncated normal distribution,  $s \sim t\mathcal{N}(0, \sigma)$  to maintain perturbations within the bounded domain, unit square by avoiding unbounded tails. The density function for the truncated normal distribution is given by:

$$\nu(x; \mu, \sigma, a, b) = \frac{1}{\sigma} \frac{\phi(\frac{x-\mu}{\sigma})}{\Phi(\frac{b-\mu}{\sigma}) - \Phi(\frac{a-\mu}{\sigma})}, \text{ where, } \phi(z) = \frac{1}{\sqrt{2\pi}} e^{-\frac{z^2}{2}}, \Phi(z) = \frac{1 + \text{erf}(\frac{z}{\sqrt{2}})}{2}, \quad (11)$$

and we choose,  $a = 0, b = 1, x - \mu = f(y)$ .

In [Bollt & Santitissadeekorn, 2013], we interpreted the random sampling associated with Equation (6) as a Monte-Carlo integration estimate involved with projection onto basis functions, Equation (8). Now in the next sections, we will encode this same expression as a histogram based density estimator of a Bayesian interpretation of the transfer operator. This will open the door to considering a different kind of error analysis, as well as other estimators. A sample of data for the Logistic map, and a random map Logistic map perturbed by truncated normal distribution noise, is shown in Figures 1 and 2. The Figure 1 compares the sample data for the standard Logistic map and the Logistic map perturbed by truncated normal distribution noise in the  $(x_n, x_{n+1})$  plane. The data is obtained by taking  $N = 1,000$  samples of

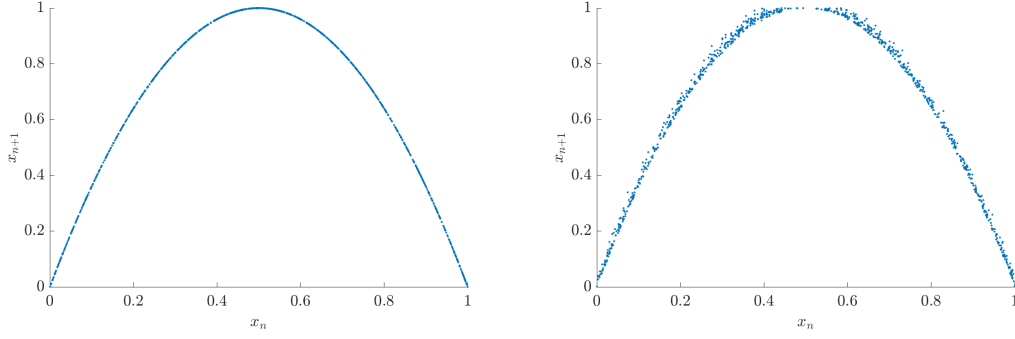


Fig. 1. The figure presents data consisting of  $N = 1,000$  samples of  $(x_n, x_{n+1})$  pairs, obtained from two different systems. The left panel shows the data obtained from the logistic map  $x_{n+1} = f(x_n) = 4x_n(1 - x_n)$ , after an initial transient, so that the sample distribution closely approximates the invariant distribution  $p_X(x) = \frac{1}{\pi\sqrt{x(1-x)}}$ . The joint distribution is a delta function,  $p_{X'X}(x', x) = \delta(x' - f(x))$ , and the orbit is plotted in the  $(x_n, x_{n+1})$  plane. On the right panel, the data is obtained from a noisy logistic map  $x_{n+1} = f(x_n) = 4x_n(1 - x_n) + s_n$ , where  $s_n$  is chosen from an independent and identically distributed (i.i.d.) truncated normal distribution with standard deviation  $\sigma = 0.02$ . The “blur” of points roughly describes the joint distribution,  $p_{X'X}(x', x) = \nu(x' - f(x))$ , where  $\nu$  is the truncated normal distribution, as shown in Equation (11). The resulting kernels are shown in Figure 2, demonstrating the differences between the two systems.

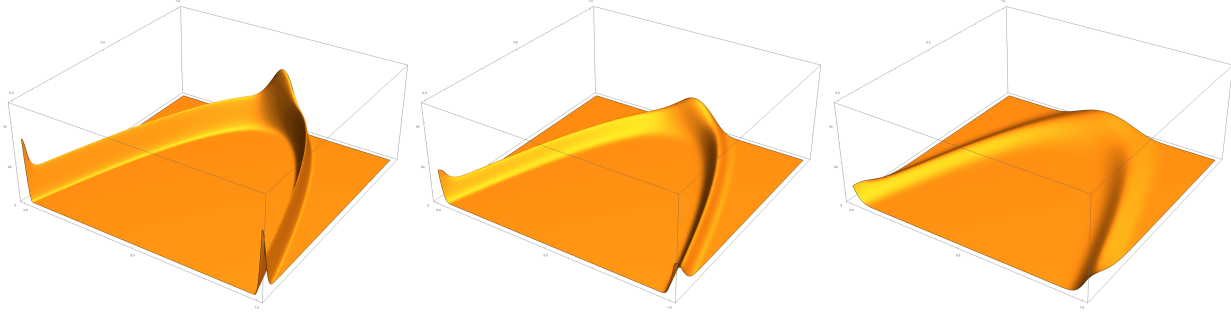


Fig. 2. This figure displays the kernel function ( $\nu$ ) of the Frobenius-Perron operator for truncated normal distribution sampling, as described in Equation (11). The figure illustrates the kernel for three different standard deviations, namely  $\sigma = 0.025$ ,  $\sigma = 0.05$ , and  $\sigma = 0.1$ . The “bumps” observed in the distribution are a direct consequence of the requirement for a bounded domain, which ensures that the distribution remains a probability distribution with a unity integral,  $\int p(x) = 1$ . Additional insights can be obtained by referring to the sample data presented in Figure 1.

$(x_n, x_{n+1})$  pairs, with the former following an initial transient to approximate the invariant distribution  $p_X(x) = \frac{1}{\pi\sqrt{x(1-x)}}$ , while the latter system is obtained by adding noise to the standard Logistic map. Figure 2 further discusses the kernel of the Frobenius-Perron operator for the Logistic map perturbed by truncated normal distribution noise. The kernel is shown for different standard deviations, namely  $\sigma = 0.025$ ,  $\sigma = 0.05$ , and  $\sigma = 0.1$ , and reveals the distinctive “bumps” observed in the distribution. These bumps are a direct result of the bounded domain requirement, which ensures that the distribution remains a probability distribution with a unity integral,  $\int p(x) = 1$ . The insights obtained from this figure provide a better understanding of the effect of noise perturbations on the dynamics of the system. An Ulam-Galerkin estimate of the stochastic matrices Equation (8) are shown in Figures 3 and 4, with further interpretation as a histogram estimator as described in the next section of corresponding Bayesian estimators.

### 3. Bayesian Interpretation of the Transfer Operator

The Frobenius-Perron operator can be interpreted in a Bayesian context in the following manner. Let us denote the output-input pair of the function  $f$  by  $(x', x)$ , where  $x' = f(x)$ , and consider these pairs as samples of the random variables  $X$  and  $X'$ . Note that  $X'$  is a transformed version of the random variable  $X$  under the function  $f$ . Considering, a statement of conditional and compound densities leads

to an interpretation of the Frobenius-Perron operator as a Bayes update. Reviewing, the joint density,  $p_{X'X}(x', x)$ , of random variables  $X'$  and  $X$  marginalizes to,

$$p_{X'}(x') = \sum_{x: x'=f(x)} p_{X'X}(x', x) = \sum_{x: x'=f(x)} \frac{p_X(x)}{|Df(x)|}, \quad (12)$$

in terms of the summation over all pre-images of  $x'$ . Notice that the middle term is written as a marginalization across  $x$  of all those  $x$  that lead to  $x'$ . This Frobenius-Perron operator, as usual, maps densities of ensembles under the action of the map  $f$ . Comparing to the defining statement of a conditional density in terms of a joint density,

$$p_{X'X}(x', x) = p_{X'|X}(x'|x)p_X(x). \quad (13)$$

We reinterpret, in the noiseless case,

$$p_{X'|X}(x'|x) = \frac{1}{|Df(x)|} \delta(x' - f(x)). \quad (14)$$

In the language of Bayesian uncertainty propagation,  $p_{X'|X}(x'|x)$  describes a likelihood function, interpreting future states  $x'$  as data and past states  $x$  as parameters, by the standard Bayes phrasing,

$$p(\Theta|\text{data}) \propto p(\text{data}|\Theta) \times p(\Theta), \quad (15)$$

for parameter  $\Theta$ , or simply by standard names of the terms,

$$\text{posterior} \propto \text{likelihood} \times \text{prior}. \quad (16)$$

From a Bayesian perspective, we can interpret the elements of the matrix approximation  $\mathbf{P}$  in a manner analogous to Equation 5. Specifically, the elements  $\mathbf{P}_{i,j}$  can be regarded as a matrix of likelihood functions, given by:

$$\mathbf{P}_{i,j} = P(x \in B_i | x' \in B_j) = \frac{P(x \in B_i, x' \in B_j)}{P(x \in B_i)} = \frac{m(B_i \cap f^{-1}(B_j))}{m(B_i)}. \quad (17)$$

Here,  $m(B_i)$  represents the prior probability of  $B_i$ , and  $m(B_i \cap f^{-1}(B_j))$  represents the joint probability of  $B_i$  and the pre-image of  $B_j$  under the transformation  $f$ . By comparing this interpretation to that of Equation 5, we can see that the matrix  $\mathbf{P}$  can be thought of as a set of conditional probabilities that quantify the likelihood of transitioning from one bin to another under the transformation  $f$ . Furthermore, the standard Ulam estimator, Equation (6), can be taken as a histogram method to estimate, the joint and marginal probabilities,  $p_{X'X}$  and  $p_X$  by occupancy counts in the related boxes,  $B_i$  and  $B_j$  with,

$$\begin{aligned} P(x \in B_i, x' \in B_j) &\sim \#x_n \in B_i, x_{n+1} \in B_j, \text{ and,} \\ P(x \in B_i) &\sim \#x_n \in B_i. \end{aligned} \quad (18)$$

The conditional follows by division, to the estimator of the matrix  $\mathbf{P}_{i,j}$  describing the likelihood function. In these terms, we are positioned to describe the statistical error of expressions such as Equation (6) for the matrix  $\mathbf{P}_{i,j}$  estimator of the Frobenius-Perron operator, by the theory of density estimators, for  $p_{X'X}(x', x)$  and  $p_X(x)$  respectively. First, in the next section, we will discuss this histogram estimator, and then in following sections, we will consider other estimators, notably the KDE.

## 4. Theory of Density Estimation

As we have argued in the previous section, the problem of estimation of an Ulam-Galerkin estimator of the Frobenius-Perron operator is equivalent to the Bayes computation of the conditional density  $p_{X'|X}(x'|x)$ , derived by histogram estimators of the joint and marginal densities,  $p_{X'X}(x', x)$ ,  $p_X(x)$ , respectively. Therefore in this section, we review what is classical theory from the statistics of density estimation, found in many excellent textbooks, such as [Silverman, 1999; Scott, 2015]. First we will review some details of histogram estimators, considering the central issues bias, variance and choice of bandwidth. Then in the

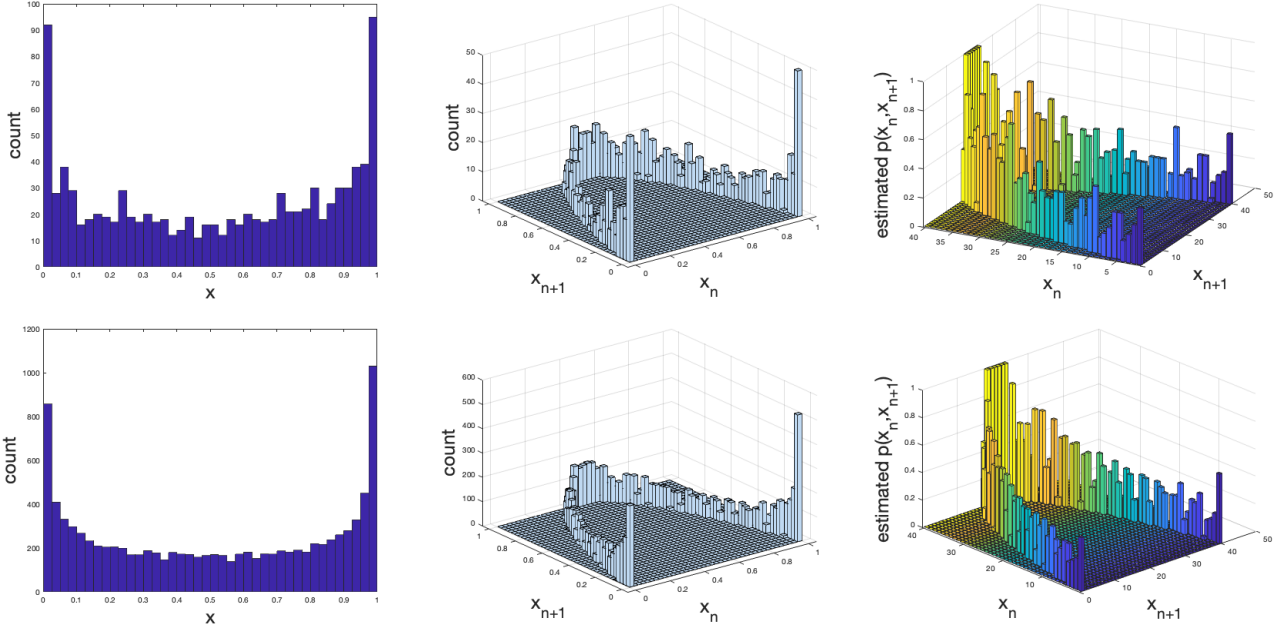


Fig. 3. The top row of this figure presents histogram estimates of the marginal, joint, and conditional distributions  $p_X(x)$ ,  $p_{X'X}(x', x)$ , and  $p_{X'|X}(x'|x)$  of the  $N = 1,000$  sample orbit shown in Figure 1. The bandwidth used for estimation is  $K = 40$ , and the joint distribution estimate uses a grid of  $40 \times 40$  cells. The rightmost estimate,  $p_{X'|X}(x'|x)$ , obtained by Equations (5), (6), (8), (17) and (18) is an Ulam-Galerkin estimate of the Frobenius-Perron operator and can be understood as a transition matrix. The bottom row of this figure presents a longer orbit of  $N = 10,000$  iterates, providing a better and smoother estimate of the true distributions with less variability. The true distribution is obtained by sampling the truncated normal distribution  $t\mathcal{N}$ , as shown in Figure 2. Comparing the estimated distributions to the true distribution provides insights into the effectiveness of the estimation techniques used in this study.

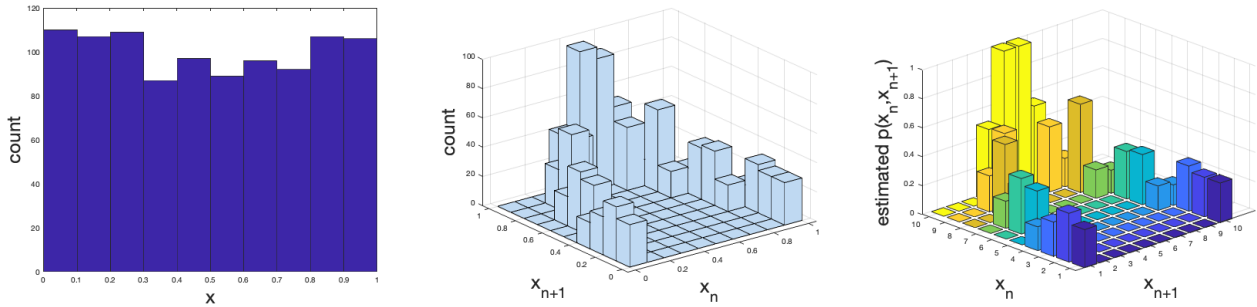


Fig. 4. The histogram distribution estimates in this figure are similar to those presented in Figure 3, but the  $N = 1,000$  data points for  $x$  were obtained i.i.d. from a uniform distribution, as opposed to being sampled from an orbit. Marginal, joint, and conditional distributions  $p_X(x)$ ,  $p_{X'X}(x', x)$ ,  $p_{X'|X}(x'|x)$  are estimated, however more coarsely (wider bandwidth for less variability, more bias (smoothing)) with  $K = 10$  and  $10 \times 10$  cells respectively. contrast to the true distribution shown in Figure 2, sampled by truncated normal  $t\mathcal{N}$ .

subsequent subsection, we will re-cast the problem as one of KDE, for which those same three issues, bias, variance and bandwidth, suggest some advantages for KDE.

For each, we state a general random variable  $X$  that is distributed by  $p_X(x)$ , but for simplicity of presentation in this section, we assume a unit interval,  $x \in [0, 1]$ , and so is the support of  $p_X(x)$ . Likewise, assume  $(x', x) \in [0, 1] \times [0, 1]$ , and  $p_{X'X}(x', x)$  has support in the unit square. The standard theory of density estimation also assumes a smooth density function [Silverman, 1999; Scott, 2015; Fan & Gijbels, 2018],  $|p'_X(x)| \leq C_1$  and  $|Dp_{X'X}| \leq C_2$ , for constants of uniform bound,  $C_1, C_2 \geq 0$ . Note however, this is already a problem regarding perhaps the most popular example for pedagogical study, the invariant density

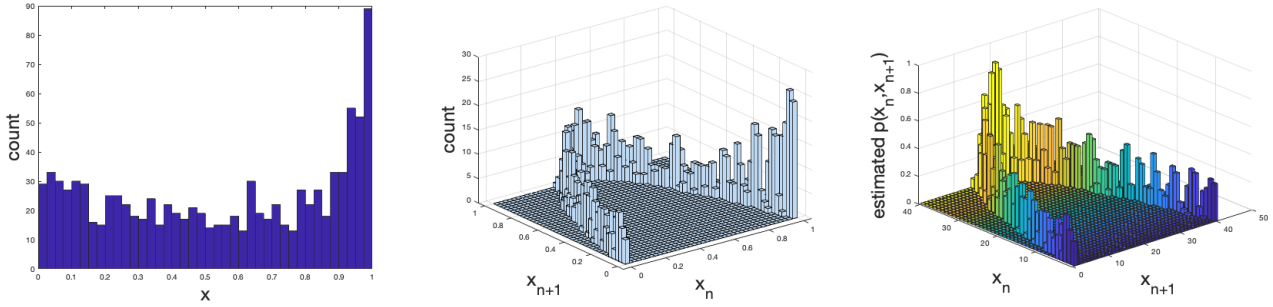


Fig. 5. Histogram distribution estimates, as Figure 4, of  $p_X(x)$ ,  $p_{X'|X}(x'|x)$ ,  $p_{X'|X}(x'|x)$ , but of the random Logistic map orbit data by truncated normal distribution noise,  $\sigma = .02$  the orbit data shown in Figure 1. These plots are similar in variability vs bias (smoothing) character as the no noise scenario of Figure 4(Top Row) even with the same smoothing, despite the differences of the true underlying distribution as the kernel cannot distinguish these properties. However, it is interesting that the marginal distribution estimating the invariant distribution is clearly different contrast to the true distribution shown in Figure 2, sampled by truncated normal  $t\mathcal{N}$ .

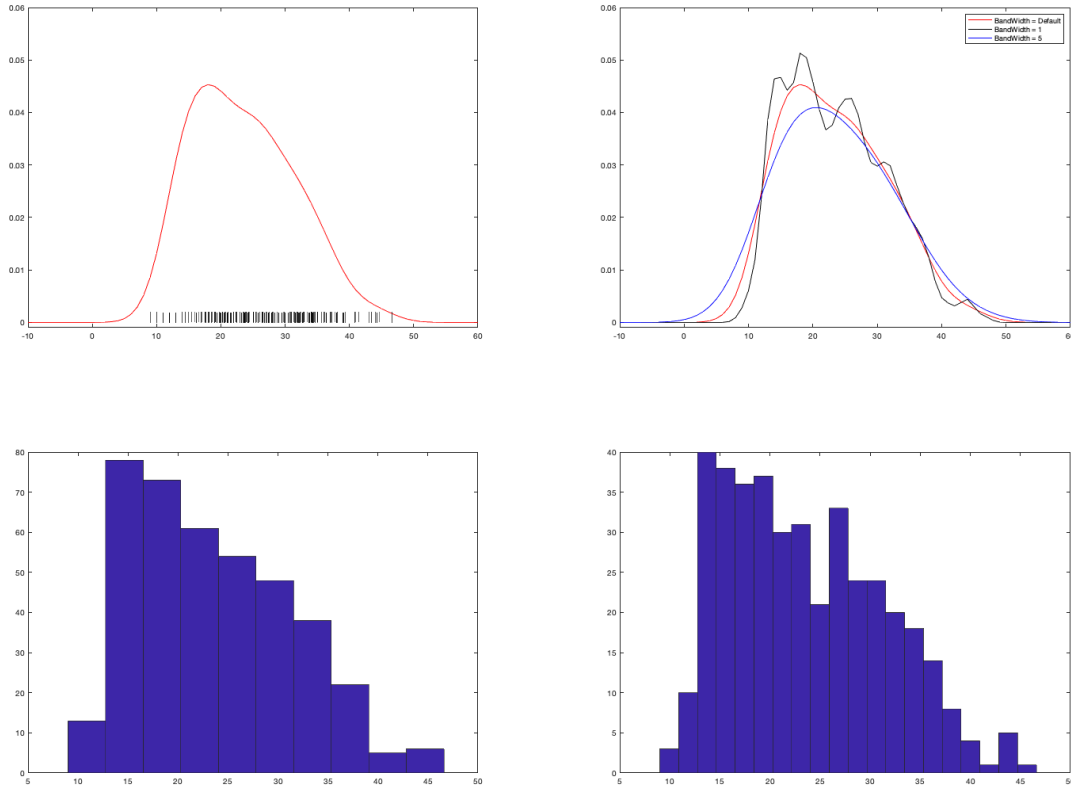


Fig. 6. The top row of figures shows the KDE estimation using the Gaussian kernel for a given data set (generated using the Chi-squared distribution for the purposes of this demonstration). The top right figure contrasts the estimation with the kernel bandwidth. The bottom row demonstrates the density estimation for the same data set using the histogram estimation method. Additionally, the bottom left and right figures contrast the estimation with the bin size.

of the logistic map is  $p_x(x) = \frac{1}{\pi\sqrt{x(1-x)}}$ , is unbounded and has unbounded derivative,  $p'_X(x) = \frac{2x-1}{2\pi\sqrt{x(1-x)}^3}$ . Likewise, Markov and semi-Markov maps will not generally have smooth densities as called out as necessary



conditions for application of the estimation theory bounds. However, like the density of the true Logistic map, these too have smooth densities when the noisy, meaning additive noise at each step variant of the mapping is used, and its corresponding transfer operator. Nonetheless, many have made practice of presenting the invariant distribution as estimated from sample orbits, Figure 3(Left). Additionally, there exist numerical techniques for selecting an appropriate bandwidth in order to mitigate the challenges associated with boundary effects [Sheather & Jones, 1991].

The key issue in any estimator is accuracy, versus the amount of data available. Generally, we want an analysis of MSE of the estimator, which requires both bias and variance, since  $\text{MSE} = \text{bias}^2 + \text{Var}^2$ .

#### 4.1. Theory of Density Estimation Using Histograms

Here we review density estimation, closely following [Scott, 2015], first in one dimension, and then the multivariate scenario.

Considering a unit interval,  $[0, 1]$ , it may be divided into  $K$  cells (bins),

$$\mathcal{B} = \{B_i\}_{i=1}^K, B_i = \left[\frac{i-1}{K}, \frac{i}{K}\right), i = 1, 2, \dots, K, \quad (19)$$

which is a uniform topological partition, meaning interiors are mutually disjoint and the union closure covers (both closed under taking unions and closures, and also forms a cover). Similarly, a multivariate histogram is a topological partition into bins, usually rectangles (but other shapes, especially tessellations are not uncommon). Otherwise, we are continuing with the discussion of the single variate estimator. Given a sample  $\{x_n\}_{n=1}^N$  and a set of bins  $\{B_j\}_{j=1}^K$ , the Histogram Density Estimation (HDE) for the random variable  $X$ ,  $\overline{p_{N,K}}(x_i)$ , which approximates  $p(x_i)$ , for any  $x_i \in B_i$ , is given by

$$\overline{p_{N,K}}(x_i) = \frac{\#x_n \in B_i}{N} \times \frac{1}{m(B_i)} = \frac{K}{N} \sum_{j=1}^N \xi_{B_i}(x_j), \quad (20)$$

where  $\#x_n \in B_i$  is the number of observations in bin  $B_i$ ,  $N$  is the total number of observations,  $m(B_i)$  is the measure of bin  $B_i$ , and  $\xi_{B_i}(x_j)$  is the indicator function that takes the value 1 if  $x_j$  belongs to bin  $B_i$  and 0 otherwise.

The key part of density estimators is the analysis of the bias of the estimator, [Scott, 2015], continuing with  $\overline{p_{N,K}}(x_i)$  for a point  $x_i \in B_i$  that need not be assume to be one of the data points  $x_j$ . Consider the probability that the sample  $x_j \in B_i$ ,  $P(x_j \in B_j)$ ,

$$\mathbb{E}(\overline{p_{N,K}}(x_i)) = \mathbb{E}(KP(x_j \in B_j)) = K \int_{\frac{i-1}{K}}^{\frac{i}{K}} p_X(s) ds = p_X(\tilde{x}), \text{ for } \tilde{x} \in B_j, \quad (21)$$

by mean value theorem and fundamental theorem of calculus. Therefore, the bias of the estimator is,

$$\text{bias}_{hist}[\overline{p_{N,K}}(x)] = \mathbb{E}(\overline{p_{N,K}}(x) - p_X(x)) = p_X(\tilde{x}) - p_X(x) \leq |p'_X(\hat{x})| |\tilde{x} - x| \leq \frac{C_1}{K}. \quad (22)$$

The first inequality follows again by the mean value theorem, this time for a value  $\hat{x} \in (x, \tilde{x})$  (or perhaps the opposite order), and by product of absolute values, and the fact that  $\tilde{x}, \hat{x} \in B_i$ . Furthermore, it should be noted that the issue of bias in HDE (see Equation (22)) involves a trade-off between limiting the derivative of the density function  $p'_X \leq C_1$  and selecting an appropriate number of bins  $K$  to obtain a desirable level of accuracy.

The variance can be computed with Equation (20),

$$\begin{aligned} \text{Var}_{hist}(\overline{p_{N,K}}(x)) &= K^2 \text{Var}\left(\frac{K}{N} \sum_{j=1}^N \xi_{B_i}(x_j)\right) \\ &= \frac{K^2 P(x_j \in B_i)(1 - P(x_j \in B_i))}{N} = \frac{K^2 \left(\frac{p_X(\tilde{x})}{K}\right) \left(1 - \frac{p_X(\tilde{x})}{K}\right)}{N} \\ &= \frac{K p_X(\tilde{x}) + p_X^2(\tilde{x})}{N} \end{aligned} \quad (23)$$

Variance is a question of balancing the number of bins  $K$  versus the data count  $N$ , but relative to the unknown density  $p_X$ .

Therefore the mean square error for the density estimation  $p_{N,K}(x)$  at an arbitrary point  $x \in [0, 1]$  follows,

$$\text{MSE}_{hist}(\overline{p_{N,K}}(x)) = \text{bias}_{hist}^2(\overline{p_{N,K}}(x)) + \text{Var}_{hist}(\overline{p_{N,K}}(x)) \leq \frac{C_1^2}{K^2} + \frac{Kp_X(\tilde{x}) + p_X^2(\tilde{x})}{N}. \quad (24)$$

To interpret, when a fixed data set (size)  $N$  is given, from an unknown distribution  $p_X$ , we can only choose  $K$  and this choice is called bandwidth selection. From Equation (24), large  $K$  (more bins) yields decreased bias (the first term), but the variance (the second term) will tend to be large. Thus demonstrates the balancing struggle between bias and variance in choosing the number of bins, the bandwidth. Figs. 3-5 demonstrate this bandwidth selection balancing act. Again, we reiterate that formally the analysis requires  $C_1 \geq 0$  be bounded whereas the derivative of the invariant density of the logistic map is not of bounded derivative type in  $[0, 1]$ , still many estimates exist in the literature ([Hall & Wolff, 1995; Bollt, 2000; Nie & Coca, 2018] etc.), including ourselves, which we now call a “typical sin.” An argument that it may not be fatal for practical problems is the fact that in real world dynamical systems that there is always noise, which has the effect of smoothing (e.g., noise sampled from a smooth distribution serves as a mollifier that can bring even a singular distribution “blurred” into a  $C^\infty$  distribution) or rather producing invariant densities that are smooth after all [Petersen, 1989; Robinson, 1998; Dajani & Kraaikamp, 2002; Becker & Dörfler, 1989; Tu, 2012]. See Figure 3 for histogram density estimations for the Figure 1(Right) randomly perturbed logistic map data.

Note that analysis of MSE in the theory of multivariate histogram estimators is similar in methodology, to which we refer to [Scott, 2015]. The important point to this stage of the paper is that the famous Ulam-Galerkin estimation of the transfer operators by formula Equation (6) amounts to problems of density estimations of the marginal and joint distributions  $p_X(x)$  and  $p_{X'|X}(x', x)$  leading to the estimation of the conditional distribution  $p_{X'|X}(x'|x)$ . This said, we can now contrast that this discussion is not a description of the Ulam problem (vs the Ulam-Galerkin estimation), since the Ulam problem describes that these estimates are stochastic matrices each with dominant eigenvector describing the invariant state of the corresponding Markov chain, and that converges weakly to the invariant distribution of the original dynamical system; and conditions for when this is in fact true were given as a theorem under hypothesis of bounded total variation first in [Li, 1976].

Now we pursue to other, perhaps more favorable density estimators of the transfer operator, notably KDE.

## 4.2. Theory of KDE

Another major category of data-driven nonparameteric density estimators is the KDE. It is a data-driven estimator based on mixing simpler densities. These are defined in terms of a kernel function,  $\mathcal{K}$ , which is itself a real density function. Stating for single-variate data,  $\mathcal{K} : \mathbb{R} \times \mathbb{R} \rightarrow \mathbb{R}^+$ , and such that: 1)  $\mathcal{K}(x)$  is symmetric, 2)  $\int_{\mathbb{R}} \mathcal{K}(x)dx = 1$ , 3)  $\lim_{x \rightarrow \pm\infty} \mathcal{K}(x) = 0$ . These are sufficient to guarantee that the KDE estimator built out of convex sums of sampling  $\mathcal{K}$  at data points, itself is a density,

$$\overline{p_{N,\delta}}(x) = \frac{1}{\delta N} \sum_{i=1}^N \mathcal{K}\left(\frac{x_i - x}{\delta}\right), \quad (25)$$

where  $\delta > 0$  is the bandwidth that controls the range or extent of influence of a given data point  $x_i$  and is a primary parameter choice, just as was the bin size for the histogram method.

There are several popular kernels, including notably, uniform, triangular, Epanechnikov, Gaussian, and quadratic kernels [Silverman, 1999; Sheather & Jones, 1991; Petersen, 1989]. These may be chosen with specific properties in mind, such as a kernel with compact support, or otherwise, Equation (11) truncated distributions in general. If  $\mathcal{K}$  is given with a compact support, then  $\mathcal{K}(x) = 0$  for values of  $x$  lying outside the support. Throughout this article, we employ the Gaussian kernel for numerical demonstrations.

Similarly, for multivariate data,  $\overline{p_{N,\Sigma}}(x) = \frac{1}{N} \sum_{i=1}^N \mathcal{K}_\Sigma(x_i - x)$ , using the common compact “scaled” kernel notation, and  $\mathcal{K}_\Sigma(z) = |\Sigma^{-1/2}|K(\Sigma^{-1/2}z)$  which for the most commonly used Gaussian kernel,  $K(z) = (2\pi)^{-d/2} \exp(-z^T z/2)$ . The matrix  $\Sigma$  serves the role of a variance-covariance in the case of a Gaussian with mean  $x_i$ .

A crucial difference is whereas histograms are centered on spatial positions, the location of the bins, and data would occupy those positions, a KDE is centered only where there is data. This can be a real savings when considering sparsely sampled data from a distribution with a relatively small support, especially in higher dimensions where the curse of dimensionality prohibits covering the space with boxes, many of which may be empty of data if the support of the density zero (no observations or data points in a region or subset).

To analyze MSE, we must again state the bias and variance of the estimator. The bias of the estimator is given by,

$$\begin{aligned} \text{bias}_{kde}(\overline{p_{N,\delta}}(x)) &= \mathbb{E}\left(\frac{1}{\delta N} \sum_{i=1}^N \mathcal{K}\left(\frac{x_i - x}{\delta}\right) - p_X(x)\right) \\ &= \frac{1}{N} \int \mathcal{K}\left(\frac{y - x}{\delta}\right) p(y) dy - p_X(x) = \int \mathcal{K}(z) p(x + \delta z) dz - p_X(x). \end{aligned} \quad (26)$$

By substituting a Taylor series,  $p(x + \delta z) = p_X(x) + \delta z p'_X(z) + \frac{1}{2} \delta^2 z^2 p''_X(x) + \mathcal{O}(\delta^2)$ , it follows [Scott, 2015] that,

$$\text{bias}_{kde}(\overline{p_{N,\delta}}(x)) = \frac{c}{2} \delta^2 p''_X(x) + \mathcal{O}(\delta^2), \quad (27)$$

where  $c = \int z^2 \mathcal{K}(z) dz$  is the second moment of the kernel and  $\mathcal{O}(\cdot)$  is the Big-O notation that shows the convergence rates.

Analysis of variance follows similarly. It can be determined by the following calculation:

$$\text{Var}_{kde}(\overline{p_{N,\delta}}(x)) = \text{Var}\left(\frac{1}{\delta N} \sum_{i=1}^N \mathcal{K}\left(\frac{x_i - x}{\delta}\right)\right) \leq \frac{1}{\delta^2 N} \mathbb{E}(\mathcal{K}^2\left(\frac{x_i - x}{\delta}\right)) \quad (28)$$

$$= \frac{1}{\delta N} \int \mathcal{K}^2(y) (p_X(x) + \delta y p'_X(x) + \mathcal{O}(\delta)) dy = \frac{1}{\delta N} (p_X(x)) \int \mathcal{K}^2(y) dy + \mathcal{O}(\delta) = \frac{1}{\delta N} p_X(x) d + \mathcal{O}\left(\frac{1}{\delta N}\right), \quad (29)$$

with  $d = \int \mathcal{K}^2(y) dy$ .

The MSE for the KDE can be obtained by combining Equations (27) and (28). It is expressed as:

$$\text{MSE}_{kde}(x) = \frac{c^2}{4} \delta^4 |p''_X(x)|^2 + \frac{d}{\delta N} p_X(x) + \mathcal{O}(\delta^4) + \mathcal{O}((\delta N)^{-1}). \quad (30)$$

Or,

$$\text{MSE} = \mathcal{O}(\delta^4) + \mathcal{O}((\delta N)^{-1}) \quad (31)$$

moderates the MSE relative to bandwidth  $\delta$  choice. Utilizing Equation (30) and its derivation process discussed earlier, it can be observed that the bias-variance trade-off in KDE can be explained by treating the bandwidth  $\delta$  as a parameter, where bias dominates for larger values of  $\delta > 0$  that are proportional to  $p''_X(x)$  (i.e., curvature), and variance dominates for smaller values of  $\delta$  that play the role of bandwidth selection.

### 4.3. Optimal MSE

The choice of bandwidth tailored to a given data set size is the key question in using a given nonparametric estimator. Despite the fact that the considerations for both histogram and kernel density estimation encompass unknown constants that rely on  $p_X(x)$  or its derivatives and are beyond our grasp due to the

absence of knowledge about  $p$  (as we may only possess data and not the true distribution), we are only able to make conclusions based on the size of the dataset and the bandwidth utilized.

$$\text{MSE}_{hist}(\overline{p_{N,K}}(x)) \sim \mathcal{O}\left(\frac{1}{K^2}\right) + \mathcal{O}\left(\frac{K}{N}\right), \quad (32)$$

but for KDE,

$$\text{MSE}_{KDE}(\overline{p_{N,K}}(x)) \sim \mathcal{O}(\delta^4) + \mathcal{O}\left(\frac{1}{\delta N}\right), \quad (33)$$

each balances large bias when the bandwidth is too large, versus large variance when the bandwidth times data set size is too small, but at different rates. The asymptotic mean square error can be shown [Silverman, 1999; Scott, 2015] to be optimal when,

$$\delta_{opt;KDE} = \frac{C}{N^{1/5}}, \quad (34)$$

where  $C$  is a constant related to the unknown density function,  $C = \frac{4p(x)d}{c^2|p''(x)|^2}$ . Similarly, for histograms, an optimal bandwidth selection is described by,

$$K_{opt;hist} = \left(\frac{NC_1^2}{p(\tilde{x})}\right)^{\frac{1}{3}}, \quad (35)$$

(and note that bandwidth for a histogram is considered to be as  $1/K$ ). So we see that asymptotically, cubic versus quintic scaling and the KDE may be better when best used (optimal bandwidth), but in practice that also depends on the constants, and one depends largely on the  $p_X$  and the other also on  $p_X''$ . The most relevant quantity when choosing a method is that for a KDE, MSE when using the optimal bandwidth is, [Scott, 2015]

$$\text{MSE}_{\delta_{opt;KDE}}(\overline{p_{\delta,N}}(x)) = \mathcal{O}\left(\frac{1}{N^{\frac{4}{5}}}\right). \quad (36)$$

However, all we can do is selection in practice, since we will not know  $p_X$ , is to inspect the scaling. Beyond 1-dimensional density estimation, multivariate KDE has a slower bandwidth rate [Scott, 2015] ,

$$\delta_{opt;KDE} = \frac{C}{N^{\frac{1}{4+D}}}, \quad (37)$$

in  $D \geq 1$  dimensions. For example, the density estimation problem associated with  $p_X(x)$  is  $D = 1$  for a transfer operator of the logistic map, but the joint density  $p_{X'X}(x', x)$  is  $D = 2$  for the same.

One may utilize either a heuristic rule-of-thumb approach or a systematic optimization method [Silverman, 1999] to determine the optimal parameter values for density estimation. In this demonstration, as we possess precise knowledge of the density function, we will employ the UB to exemplify the optimal parameter values.

## 5. Results and Discussion

In this section, we focus on estimating the Frobenius-Perron operator by using the previously discussed density estimation methods. In other words, we calculate the  $\mathbf{P}$  matrix in Equation (17) by density estimation methods. We use the logistic map example to demonstrate the results. In this demonstration, uniformly distributed  $N = 10^6$  initial conditions were used and evolved using a logistic map  $x' = 4x(1 - x)$  for a relatively long time which was used to approximate the invariant density  $\rho(x) = \frac{1}{\pi\sqrt{x(1-x)}}$ . Now our goal is

to estimate the Frobenius-Perron operator by evaluating the probability density function  $p(x'|x) = \frac{p(x,x')}{p(x)}$ . For this calculation, we estimated the  $p(x)$  and the joint probability density  $p(x, x')$  by using the data through density estimation methods. In this section, we analyze the estimation of the  $p(x)$  by the density estimation methods in detail and compare it to the theoretical explanation in the section 4. Then we demonstrate the estimation  $\mathbf{P}$  matrix of the Frobenius-Perron operator by discretized probability density function  $p(x'|x)$ .

### 5.1. Histogram Estimation vs KDE for logistic map example

Histogram Estimation is based on the number of samples ( $N$ ) and the number of bins ( $K$ ) (See details in section 4. Here, we demonstrate the effect of the bin size. The estimation of the invariant density  $\rho(x)$  by the histogram method is denoted by  $\bar{\rho}_{N,K}$ . Figure 7 shows the changes in the estimation with parameter  $K$ . Since the true density is known, the MSE and the UB of the MSE can be calculated for this example by Equation (24). Note that the notations

$$\begin{aligned} \text{MSE} &= (\rho(x) - \bar{\rho}_{N,K}(x))^2 \\ \text{UB} &= C_1^2 \frac{1}{K^2} + \frac{\rho(\hat{x})}{N} K + \frac{\rho^2(\hat{x})}{N} \end{aligned}$$

are from the Equation (24) and depends on the true density function  $\rho(x)$ . Additionally, through the examination of the UB and MSE, we can determine the optimal bin size,  $K_{opt;hist}$ , as illustrated in Figure 8 and discussed in Section 4.3.

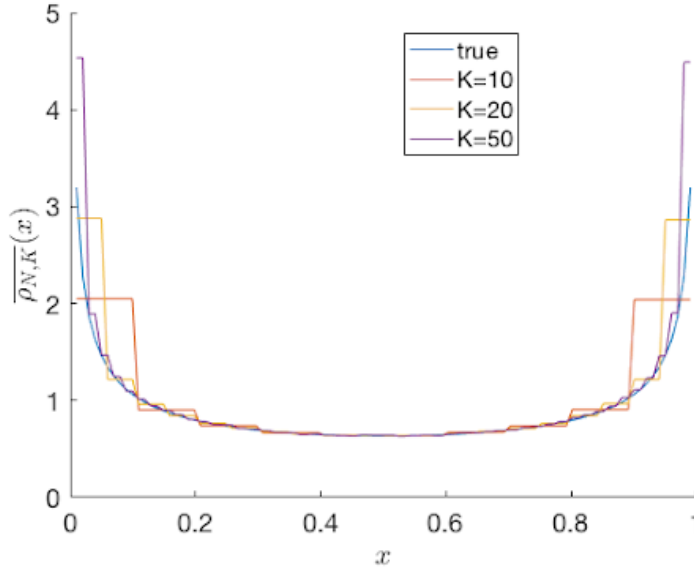


Fig. 7. The figure shows the results of histogram-based density estimation,  $\bar{\rho}_{N,K}$ , for the invariant density,  $\rho$ , of the logistic map. The impact of the number of bins,  $K$ , on the estimation  $\bar{\rho}_{N,K}$  is illustrated. The sample size used for estimation is  $N = 10^6$ . The figure provides insights into how the choice of the number of bins affects the accuracy and bias of the density estimation.

As we discussed in the Section 4.2, KDE is based on the number of data points ( $N$ ) and the kernel bandwidth ( $\delta$ ). In this section, we numerically demonstrate (employ the Gaussian kernel for these demonstrations) the effect of the bandwidth. Notice that, a change in the bandwidth will result in a change in the MSE (see Figure 9). The UB of MSE for the KDE is given in Equation (30) and the following results are calculated by the Equation (30). Error analysis and the optimal MSE is demonstrated in the Figure 10. Furthermore, note that the optimal MSE can be achieved with a bandwidth of approximately  $\delta_{opt;KDE} = 0.0011$ .

Due to the unboundedness of the density function, both estimation methods have higher estimation errors closer to the endpoints of the interval  $[0, 1]$ . In general, density estimation has issues when estimating a unboundedness probability density with finite support. Despite this limitation, the KDE method tends to have lower overall estimating error when compared to the histogram method using finite data. Figure 11 demonstrates that MSE for KDE is comparatively lower than the MSE for histogram method with their optimal parameter values.

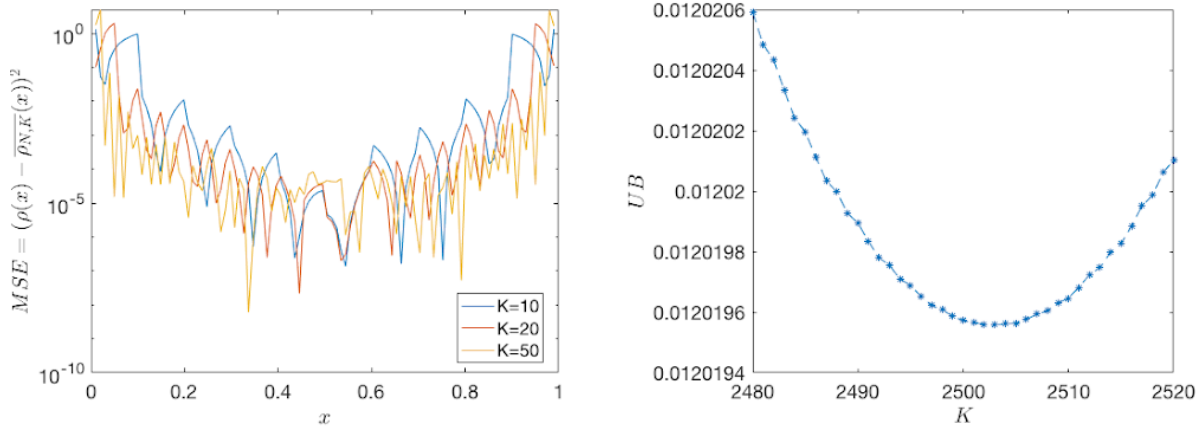


Fig. 8. The left figure displays the MSE of the estimated density function on a uniformly spaced grid of 100 points in the interval  $[0.01, 0.99]$ , as a function of the bin size  $K$ . The right figure shows the behavior of the UB with the bin size for the logistic map example. The optimal MSE can be achieved at a bin size of  $K_{opt} = 2503$ .

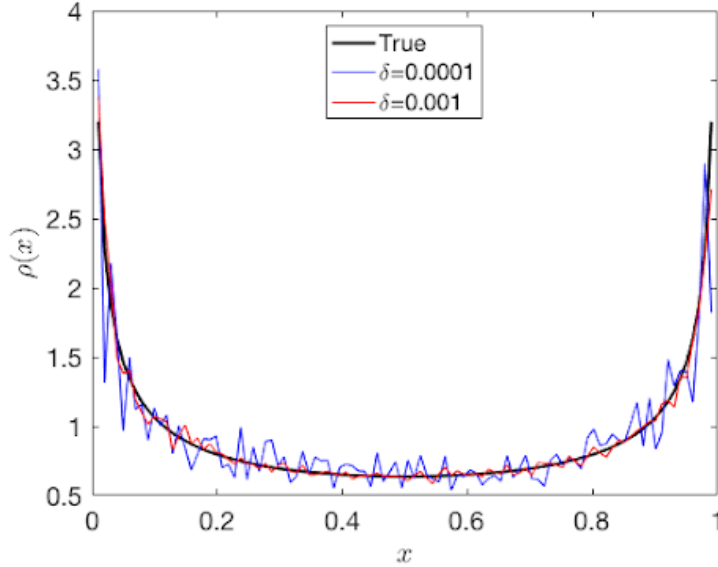


Fig. 9. The figure illustrates the KDE of the invariant density  $\rho$  of the logistic map. It depicts how the bandwidth parameter  $\delta$  affects the KDE with sample size  $N = 10^6$ .

## 5.2. Estimating the Frobenius-Perron operator

Now, we will numerically investigate the theoretical discussion presented in Section 3. We have shown the popular classical Ulam-Galerkin method as a histogram estimation of the  $p(x'|x)$ . Hence, we argued that estimating Frobenius-Perron operator through conditional probability density  $p(x'|x)$  can be extended by using any density estimation method. In this article, we presented the KDE as an alternative density estimation to the histogram method.

The finite-dimensional estimation of Frobenius-Perron operator can be represented using a matrix ( $\mathbf{P}$ ). The comparison of the estimated  $\mathbf{P}$  matrix by each method can be found in the Figure 12. Furthermore, left eigenvector corresponds to the eigenvalue 1 of the  $\mathbf{P}$  matrix can be used to estimate the invariant density of the map. Figure 13 shows the left eigenvector correspond to the eigenvalue 1 of matrix  $\mathbf{P}$  calculated by histogram and KDE method.

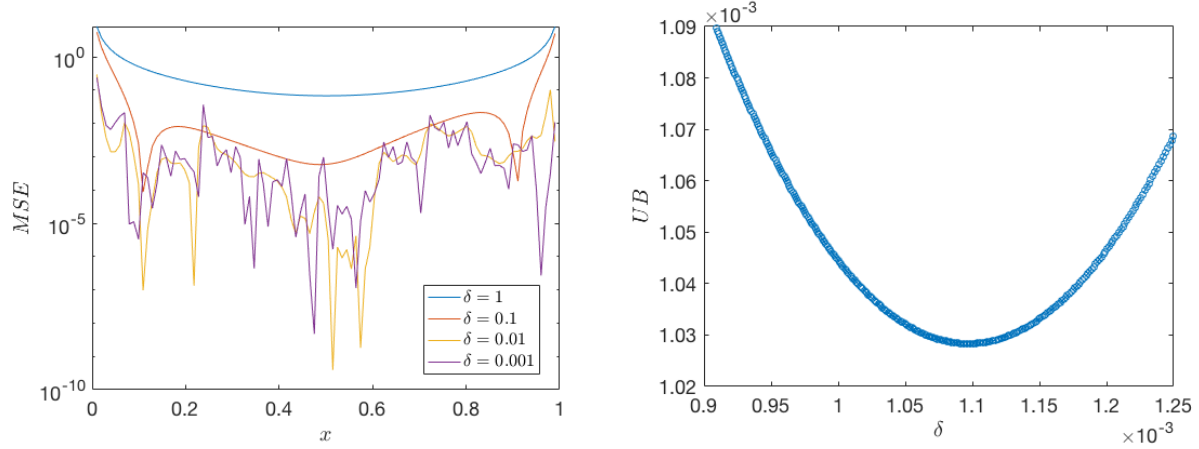


Fig. 10. The left figure displays the MSE of the estimated density function on a uniformly spaced grid of 100 points over the interval  $[0.01, 0.99]$ . It also shows how the MSE changes with the bandwidth parameter  $\delta$  for the KDE. The right figure presents the analysis of the UB and how it varies with the bandwidth parameter for the logistic map example. The optimal bandwidth can be identified at around  $\delta_{opt} = 0.0011$ .

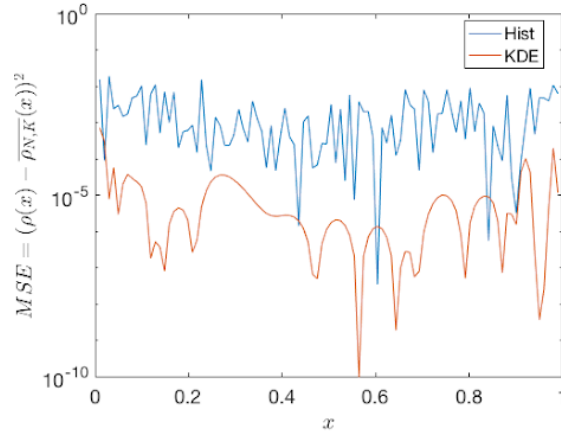


Fig. 11. This figure presents a comparison of the MSE of the histogram density estimation and KDE, both with their respective optimal parameter values  $K_{opt} = 2503$  and  $\delta_{opt} = 0.0011$ . The sample data used is the invariant density of the logistic map, with a sample size of  $N = 10^6$  and equally spaced grid points spanning the interval  $[0.01, 0.99]$ .

## 6. Conclusion

The main contribution of this paper is the probability density viewpoint to the estimating Frobenius–Perron operator that enables us to incorporate the existing rich analysis of statistical density estimation formalism to find an efficient estimator. Furthermore, the theory suggests that the KDE is more efficient than the histogram methods used in the standard Ulam method. Additionally, this paper discusses a KDE method to estimate the transition probability that estimates the Frobenius–Perron operator, from empirical time series ensemble data of a dynamical system. To date, the literature mostly used the Ulam method for estimating the transfer operator but this study offers a more accurate estimation based on KDE. Our Bayesian interpretation of the Frobenius–Perron operator is important to identify the operator in terms of conditional probability density because it allows us to bring density estimation theory into play. It is shown at the beginning of this article how the Ulam–Galerkin method can be interpreted as a histogram density estimation method. Theory and numerical results have been presented which suggest that KDE is a better approximation for estimating probability densities. Hence, it is also shown that KDE may be used for finite approximation for the Frobenius–Perron operator. Finally we showed that the KDE-based approximation is a better estimator for the operator than the histogram-based current Ulam–Galerkin method.

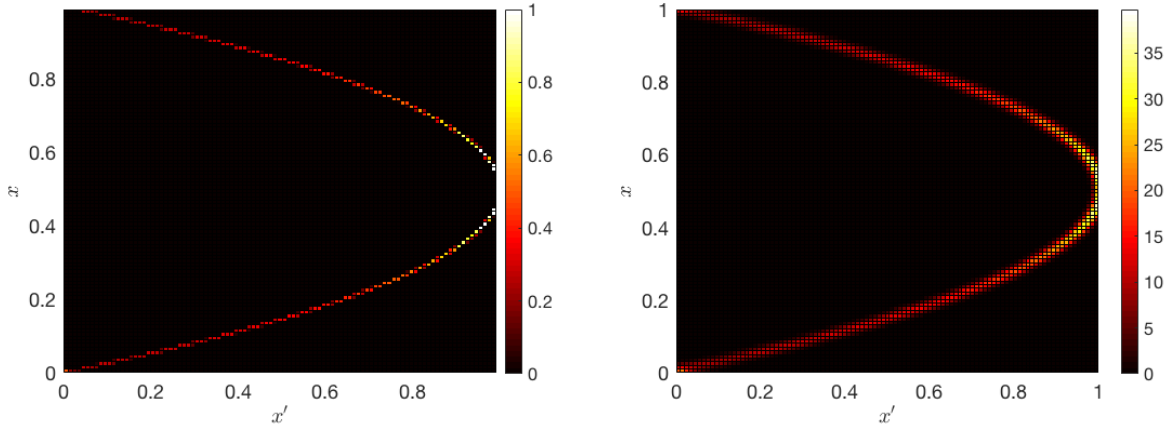


Fig. 12. This figure presents estimates of the matrix  $\mathbf{P}$ , which approximates the Frobenius-Perron operator in a finite domain, obtained using two density estimation techniques: the histogram method (left) and the KDE (with Gaussian Kernel) (right). The sample data used for the estimation consists of  $N = 10^6$  independent and identically distributed samples drawn from the uniform distribution  $X \in [0.01, 0.99]$ , and its transformation  $X' = f(X)$ , where  $f$  is the logistic map. The optimal parameter values  $K_{opt} = 2503$  and  $\delta_{opt} = 0.0011$  are chosen for the estimation. The matrix  $\mathbf{P}$  has dimensions  $K \times K$ , where  $K = 400$  is the number of bins or grid points used in the density estimation.

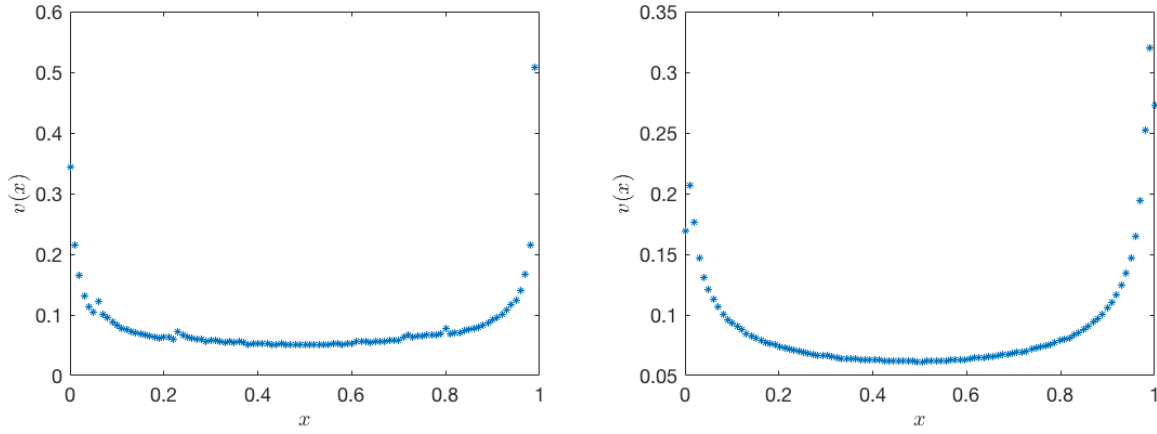


Fig. 13. The figure displays the left eigenvector of matrix  $\mathbf{P}$ , which corresponds to the eigenvalue 1 of the matrix  $\mathbf{P}$  shown in Figure 12. The left eigenvector can be used to estimate the invariant density of the logistic map. The left eigenvectors of  $\mathbf{P}$  estimated using two density estimation techniques are shown in the figure: the histogram method (left) and the kernel density estimation (KDE) (right). The sample data used to estimate  $\mathbf{P}$  is the same as in Figure 12. The matrix  $\mathbf{P}$  has dimensions  $K \times K$ , where  $K = 400$  is the number of bins or grid points used in the density estimation. The optimal parameter values  $K_{opt} = 2503$  and  $\delta_{opt} = 0.0011$  are chosen for the estimation.

As a result of conducting this research, we propose the possibility of introducing any density estimation methods to this field. It would be fruitful to pursue further research about the KDE-based estimation of the Frobenius–Perron operator for high-dimensional maps to analyze this method.



## Acknowledgments

Erik Boltt gratefully acknowledges funding from the Army Research Office (ARO), the Defense Advanced Research Projects Agency (DARPA), the National Science Foundation (NSF) and National Institutes of Health (NIH) CRNS program, and the Office of Naval Research (ONR) during the period of this work.

## Code availability

The code used in this study is available at <https://github.com/sudamphy/FPoperatorDE.git>.

## Abbreviations

**KDE** Kernel Density Estimation.

**HDE** Histogram Density Estimation.

**i.i.d.** independently and identically distributed.

## References

- Becker, K.-H. & Dörfler, M. [1989] *Dynamical Systems and Fractals: Computer Graphics Experiments with Pascal* (Cambridge University Press).
- Boltt, E. M. [2000] “Controlling chaos and the inverse frobenius–perron problem: global stabilization of arbitrary invariant measures,” *International Journal of Bifurcation and Chaos* **10**, 1033–1050.
- Boltt, E. M., Billings, L. & Schwartz, I. B. [2002] “A manifold independent approach to understanding transport in stochastic dynamical systems,” *Physica D: Nonlinear Phenomena* **173**, 153–177.
- Boltt, E. M. & Santitissadeekorn, N. [2013] *Applied and computational measurable dynamics* (SIAM).
- Boyarsky, A. & Góra, P. [1997] “Laws of chaos : Invariant measures and dynamical systems in one dimension,” .
- Chiu, C., Du, Q. & Li, T. [1992] “Error estimates of the markov finite approximation of the frobenius–perron operator,” *Nonlinear Analysis: Theory, Methods & Applications* **19**, 291–308, doi:[https://doi.org/10.1016/0362-546X\(92\)90175-E](https://doi.org/10.1016/0362-546X(92)90175-E), URL <https://www.sciencedirect.com/science/article/pii/0362546X9290175E>.
- Dajani, K. & Kraaikamp, C. [2002] *Ergodic theory of numbers*, Vol. 29 (American Mathematical Soc.).
- Dehnad, K. [1987] “Density estimation for statistics and data analysis,” *Technometrics* **29**.
- Dellnitz, M., Froyland, G. & Junge, O. [2001] “The algorithms behind gaio — set oriented numerical methods for dynamical systems,” *Ergodic Theory, Analysis, and Efficient Simulation of Dynamical Systems*, ed. Fiedler, B. (Springer Berlin Heidelberg, Berlin, Heidelberg), ISBN 978-3-642-56589-2, pp. 145–174.
- Ermann, L. & Shepelyansky, D. L. [2010] “Ulam method and fractal weyl law for perron–frobenius operators,” *The European Physical Journal B* **75**, 299–304.
- Fan, J. & Gijbels, I. [2018] *Local polynomial modelling and its applications* (Routledge).
- Froyland, G., Junge, O. & Koltai, P. [2013] “Estimating long-term behavior of flows without trajectory integration: The infinitesimal generator approach,” *SIAM Journal on Numerical Analysis* **51**, 223–247.
- Guder, R., Dellnitz, M. & Kreuzer, E. [1997] “An adaptive method for the approximation of the generalized cell mapping,” *Chaos, Solitons & Fractals* **8**, 525–534, doi:[https://doi.org/10.1016/S0960-0779\(96\)00118-X](https://doi.org/10.1016/S0960-0779(96)00118-X), URL <https://www.sciencedirect.com/science/article/pii/S096007799600118X>, nonlinearities in Mechanical Engineering.
- Hall, P. & Wolff, R. C. L. [1995] “Properties of invariant distributions and lyapunov exponents for chaotic logistic maps,” *Journal of the Royal Statistical Society. Series B (Methodological)* **57**, 439–452, URL <http://www.jstor.org/stable/2345972>.
- Hunt, F. Y. [1998] “Unique ergodicity and the approximation of attractors and their invariant measures using ulam’s method,” *Nonlinearity* **11**, 307.

- Hunt, F. Y. [2000] “Attractors, chain transitive sets and invariant measures,” *Equadiff 99: (In 2 Volumes)* (World Scientific), pp. 1042–1047.
- Junge, O. & Koltai, P. [2009] “Discretization of the frobenius–perron operator using a sparse haar tensor basis: the sparse ulam method,” *SIAM Journal on Numerical Analysis* **47**, 3464–3485.
- Klus, S., Bittracher, A., Schuster, I. & Schütte, C. [2018a] “A kernel-based approach to molecular conformation analysis,” *The Journal of Chemical Physics* **149**, 244109.
- Klus, S., Husic, B. E., Mollenhauer, M. & Noé, F. [2019] “Kernel methods for detecting coherent structures in dynamical data,” *Chaos: An Interdisciplinary Journal of Nonlinear Science* **29**, 123112.
- Klus, S., Nüske, F., Koltai, P., Wu, H., Kevrekidis, I., Schütte, C. & Noé, F. [2018b] “Data-driven model reduction and transfer operator approximation,” *Journal of Nonlinear Science* **28**, 985–1010.
- Lasota, A. & Yorke, J. A. [1982] “Exact dynamical systems and the frobenius–perron operator,” *Transactions of the american mathematical society* **273**, 375–384.
- Li, T.-Y. [1976] “Finite approximation for the frobenius–perron operator. a solution to ulam’s conjecture,” *Journal of Approximation Theory* **17**, 177–186, doi:[https://doi.org/10.1016/0021-9045\(76\)90037-X](https://doi.org/10.1016/0021-9045(76)90037-X), URL <https://www.sciencedirect.com/science/article/pii/002190457690037X>.
- Ma, T. & Bollt, E. M. [2013] “Relatively coherent sets as a hierarchical partition method,” *International Journal of Bifurcation and Chaos* **23**, 1330026.
- Mollenhauer, M., Schuster, I., Klus, S. & Schütte, C. [2020] “Singular value decomposition of operators on reproducing kernel hilbert spaces,” *Advances in Dynamics, Optimization and Computation: A volume dedicated to Michael Dellnitz on the occasion of his 60th birthday* (Springer), pp. 109–131.
- Nie, X. & Coca, D. [2018] “A matrix-based approach to solving the inverse frobenius–perron problem using sequences of density functions of stochastically perturbed dynamical systems,” *Communications in Nonlinear Science and Numerical Simulation* **54**, 248–266, doi:10.1016/j.cnsns.2017.05.011.
- Petersen, K. E. [1989] *Ergodic theory*, Vol. 2 (Cambridge university press).
- Robinson, C. [1998] *Dynamical systems: stability, symbolic dynamics, and chaos* (CRC press).
- Scott, D. W. [2015] *Multivariate density estimation: Theory, practice, and visualization* (John Wiley & Sons, Inc.).
- Sheather, S. J. & Jones, M. C. [1991] “A reliable data-based bandwidth selection method for kernel density estimation,” *Journal of the Royal Statistical Society: Series B (Methodological)* **53**, 683–690.
- Silverman, B. W. [1999] *Density Estimation for statistics and data analysis* (Chapman and Hall).
- Tu, P. N. [2012] *Dynamical systems: an introduction with applications in economics and biology* (Springer Science & Business Media).
- Tukey, J. W. [1961] “Curves as parameters, and touch estimation,” *Proceedings of the Fourth Berkeley Symposium on Mathematical Statistics and Probability, Volume 1: Contributions to the Theory of Statistics* (University of California Press), pp. 681–695.
- Tukey, P. A. & Tukey, J. W. [1981] “Graphical display of data sets in 3 or more dimensions,” *Interpreting multivariate data* **29**.
- Ulam, S. M. [1960] *A collection of mathematical problems*, 8 (Interscience Publishers).